Case study examination of the ECR structure

A helpful tool for examining the ECR structure was developed by *Vogt et al. (2009)*, who adapted well established Cluster techniques, based on four-spacecraft measurements, to three-satellite data. Since the Cluster/CIS instrument is not operational on spacecraft 2 (SC2), it is of particular interest to be able to compute gradients of plasma parameters using data only from SC1, SC3, and SC4. A first application of the new tool in computing pressure gradients, relevant for the ECR investigation and illustrated here in Figure 1, was included in *Vogt et al. (2009)*.

The pressure gradients obtained by imposing a geometric constraint, $\nabla p \parallel \mathbf{j} \times \mathbf{B}$, $\nabla p \perp \mathbf{j}$, or $\nabla p \perp \mathbf{B}$, as well as the respective work of the pressure forces, are shown on the left side of Figure 1. The three-spacecraft data allow the direct determination of the pressure gradient component in the spacecraft plane, presented in panel (c). As expected in the tail plasma sheet, its projection on the GSM *x* axis is small. In order to find the pressure gradient component normal to the spacecraft plane, an additional constraint is needed. The three geometric constraints mentioned above result in similar normal components (d, e, f). One notes that the first constraint, $\nabla p \parallel \mathbf{j} \times \mathbf{B}$, implies that ∇p is normal to both $\mathbf{j}$ and $\mathbf{B}$, therefore the results obtained provide a consistency check for the three approaches.

In the PSBL, $\mathbf{j}$ is typically dominated by the diamagnetic current carried by ions, $\mathbf{j}_d = -\nabla p \times \mathbf{B}/B^2$, and ∇p, $\mathbf{j}$, $\mathbf{B}$ are orthogonal to each other. A schematic configuration of the three vectors, that includes the

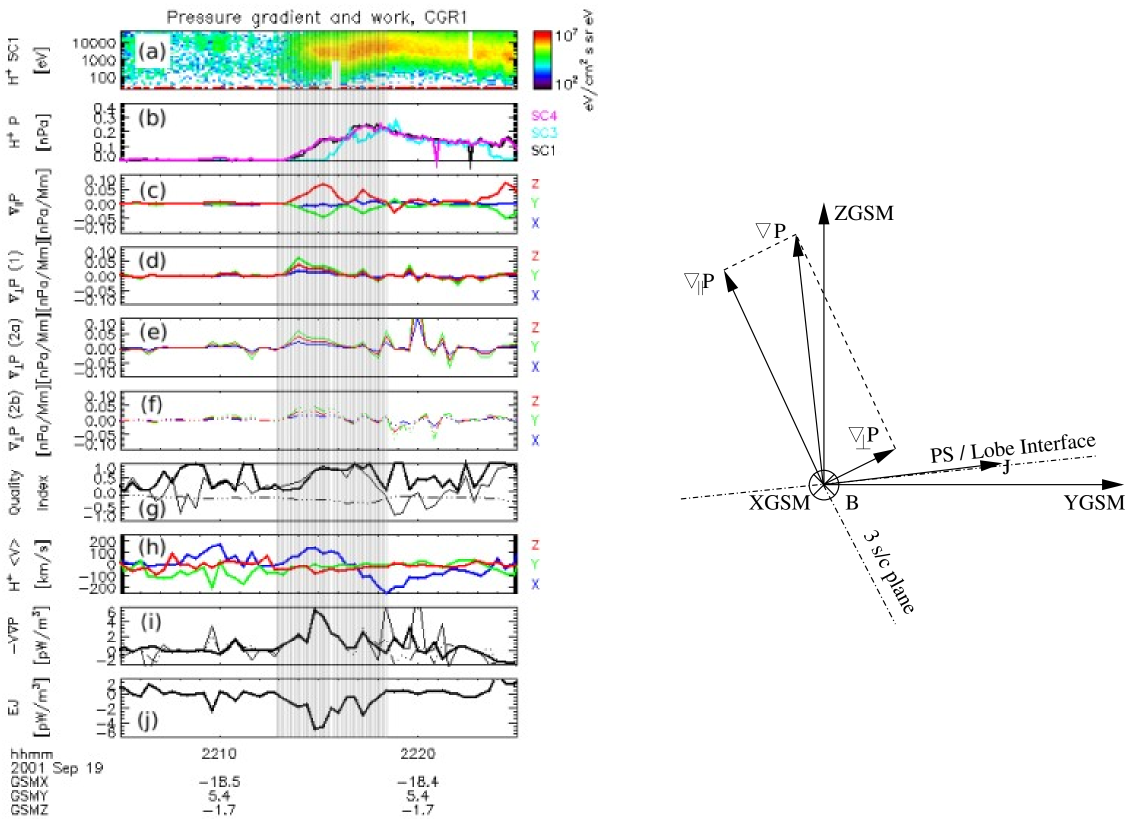

Figure 1: *Left:* Pressure gradients and the work of the pressure forces for three different geometric constraints. (**a**) H^+ energy spectrogram for SC1. (**b**) H^+ pressure for SC1 (black), SC3 (cyan), and SC4 (magenta), averaged over 24 s. (**c**) Pressure gradient parallel to the 3-spacecraft plane (SC1, SC3, SC4), $\nabla_{\parallel} p$. (**d, e, f**) Pressure gradient normal to the 3-spacecraft plane, $\nabla_{\perp} p$, computed with the geometric constraints $\nabla p \parallel \mathbf{j} \times \mathbf{B}$, $\nabla p \perp \mathbf{j}$, and $\nabla p \perp \mathbf{B}$, respectively. (**g**) Quality indices $|\hat{\mathbf{e}} \times \hat{\mathbf{n}}|^2$ (for panel (d)) and $\hat{\mathbf{e}} \cdot \hat{\mathbf{n}}$ (for panels (e) and (f)), with thick, thin, and dashed-dotted line, respectively. A quality index around zero implies the estimate of $\nabla_{\perp} p$ is not reliable. (**h**) H^+ velocity, averaged over spacecraft and over 24 s. (**i**) The work of the pressure forces, $W_K = -\mathbf{v} \cdot \nabla p$, with $\nabla p = \nabla_{\parallel} p + \nabla_{\perp} p$, corresponding to the three estimates of $\nabla_{\perp} p$. Same line styles as for the quality indices. Note the peak at 22:15 and the spikes associated with low quality indices. (**j**) The power density, $\mathbf{E} \cdot \mathbf{J}$, indicating the energy conversion rate. The energy conversion reaches a negative peak at 22:15, simultaneous with the peak in W_K, consistent with a generator process. *Right:* Parallel, perpendicular, and total pressure gradient, together with the current density, **J**, and the magnetic field (into the page), **B**. The 3-spacecraft plane and the plasma sheet / lobe interface are shown as well.

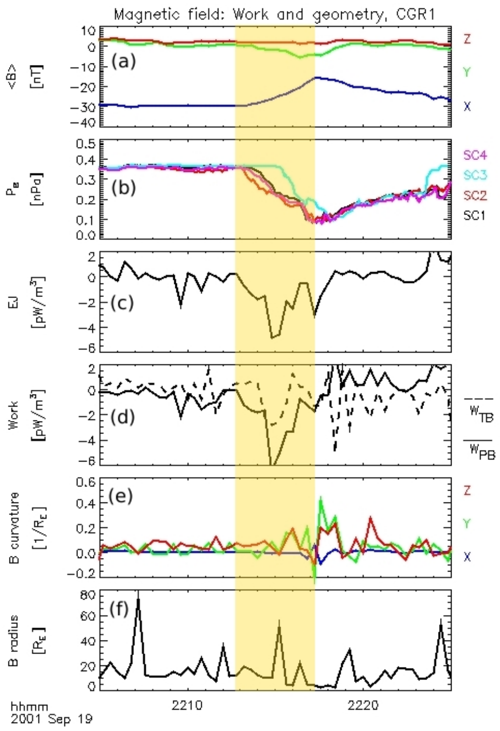

Figure 2: Work of the magnetic field forces and geometry of the magnetic field line. (**a**) Magnetic field, averaged over the Cluster spacecraft. (**b**) Magnetic pressure for each spacecraft. (**c**) Power density, $\mathbf{E}\cdot\mathbf{J}$. (**d**) Work of the magnetic pressure and magnetic stress tensor forces, W_{PB} and W_{TB}. (**e, f**) Curvature and curvature radius of the magnetic field line.

projections of the 3-spacecraft plane, and of the plasma sheet / lobe interface in the GSM (y, z) plane, is sketched on the right side of Figure 1. For simplicity, $\mathbf{B}$ is aligned with the x axis, whose tilt with respect to the spacecraft plane is neglected. The pressure gradient and its components reflect the results in the left panels and ∇p is assumed to be normal to the plasma sheet / lobe interface, which is close to the GSM (x, y) plane. The magnetic field lines thread the interface in the x direction, while the current is close to the y direction. The field-aligned component of the current does not contribute to $\mathbf{j} \times \mathbf{B}$ and to changing ∇p, therefore it is not indicated in Figure 1.

The examination of the ECR structure was extended later by evaluating the work of the magnetic field forces as well as the curvature of the magnetic field line, and the results were presented at the Cross Scale workshop (*Marghitu et al., 2009b)*. Figure 2 illustrates these evaluations for the event presented in Figure 1. Since $\mathbf{E} \cdot \mathbf{J}$ is computed by approximating $\mathbf{E}$ with $-\mathbf{v} \times \mathbf{B}$, our $\mathbf{E} \cdot \mathbf{J}$ estimate is equal to the work of the Lorentz force, $(\mathbf{J} \times \mathbf{B}) \cdot \mathbf{v}$. While theoretically the Lorentz force is the sum of a magnetic pressure term and a stress tensor term, $\mathbf{J} \times \mathbf{B} = -\nabla p_B + \nabla \cdot \mathcal{T}_B$, with $p_B = B^2/2\mu_0$ and $\mathcal{T}_B = \mathbf{BB}/\mu_0$, our $\mathbf{E} \cdot \mathbf{J}$ estimate is not equal to $W_{P_B} + W_{T_B}$ (compare panels c and d). Further investigations showed that the reason for this inconsistency was the failure of the linear approximation, underlying the computation of spatial derivatives. This reason appeared to be consistent with the large curvature (panel e) of the magnetic field line over the second half of the CGR (and at other times later on).

The work on the pressure gradients associated with ECRs generated interesting questions regarding MHD waves at the PSBL, that might be addressed in the future based on the three-spacecraft tool. Further development of three-spacecraft techniques and applications to data provided by Cluster, THEMIS, or the upcoming Swarm mission, contribute to the collaboration between ISS Bucharest and Jacobs University Bremen.